Dynamic Modeling and Simulation of Compliant Legged Quadruped Robot

M M Gor[1], P M Pathak[2]
Indian Institute of Technology Roorkee,
Roorkee, India
[1]mehulmgor@rediffmail.com,[2]pushpfme@iitr.ernet.in

J-M Yang
Kyungpook National University,
Daegu, South Korea
jmyang@ee.knu.ac.kr

A K Samantaray
Indian Institute of Technology Kharagpur,
Kharagpur, India
samantaray@mech.iitkgp.ernet.in

S W Kwak
Keimyung University,
Daegu, South Korea
ksw@kmu.ac.kr

***Abstract*—Quadruped robot has many advantages over wheeled mobile robots, but it is a discrete system in which joints of each leg has to operate in particular fashion to get the desired locomotion. So, dynamics plays an important role in the operation and control of quadruped robot. Proper conception of the dynamic formulation is must for the complex system like quadruped robot. Here, an attempt is made to generate three dimensional model of a quadruped using the bond graph technique. Bond graph is an efficient tool for system modeling from the physical model itself and various control strategies can be developed very efficiently. A quadruped robot configuration used for analysis is two links legged robot in which upper link is rigid and lower link is compliant. In a lower link, piston and piston rod is sliding inside the cylinder and movement is restricted by the internal hydraulic pressure of the cylinder which will generate compliance in the leg. Simulation of the various gait performed by the quadruped is carried out, which proves the versatility of the three dimensional model generated. The generated model can be used in research of various aspects pertaining to quadruped, the same thing is demonstrated by doing performance evaluation between compliant and rigid legged robot and also between two different gaits like trot gait and amble gait.**

***Keywords*—Quadruped robot, Bond graph, Dynamic model**

I. INTRODUCTION

Legged robot offer many advantages over wheeled robots including greater adaptability to terrain irregularities and superior off-road mobility [1, 2]. Legged systems require only a series of discrete footholds along the pathway for off-road locomotion. This property enables legged robots to traverse surfaces inaccessible to wheeled mobile robots. Compliance in the leg improves locomotion of legged robot [3]. Variable compliance in the legs [4] overcomes the size, weight, fragility and efficiency problem. Basically, legged robots are discrete system in which joint of each leg has to operate in particular fashion. So, dynamics plays an important role in the operation and control of a walking robot. Recently, there has been a noteworthy increase in the use of computational dynamics for design, analysis, simulation and control of various robotic systems. This is because of better understanding of the dynamic formulation of complex systems. To this end, various researchers used different dynamic analysis methods for multibody systems, such as the methods based on Lagrangian equation [5], Newton-Euler equation [6, 7], Kane's equation [8, 9, 10] and variational methods [11].

Benani and Giri [12] presented a dynamic model approach of quadruped considering open and/or closed kinematic chain mechanisms. It is based on Newton-Euler approach and the explicit formulation of kinematic holonomic constraints for the closed loop mechanism. Mahapatra and Roy [13] developed a dynamic model of six legged in CATIA solid modeler, SimDesigner and ADAMS multibody dynamic solver and kinematic and dynamic simulation is performed based on virtual prototyping technology. Krishnan et al. [14] presented a bond graph model of compliant legged quadruped robot in a sagittal plane. The sagittal plane dynamics have been tested through experimental set-up. Soyguder and Ali [15] solved the stance and flight phase dynamic structures in a sequential closed loop for quadruped and obtained the equation of motion for pronking gait. Shah et al. [16] presented a concept of kinematic modules for the development of the dynamic model of the four legged robots where each module is considered as a set of serially connected links. module-level Decoupled Natural Orthogonal Complement (DeNOC) matrices were introduced which helps to analyze the large number of links as a system with a smaller number of modules. Recursive kinematic relationships were obtained between two adjoining modules. Ganesh and Pathak [17] developed a dynamic model of four legged in a sagittal plane by formulating kinetic and potential energy equation of body and leg. These were used to derive Lagrangian function and then equation of motion.

In this paper, three dimensional dynamic model of compliant legged quadruped robot using bond graph has been developed. Bond graph is an efficient tool for system modeling from the physical model itself. A quadruped robot configuration used for analysis is two links legged robot in which upper link is rigid and a lower link is compliant. Lower link is considered similar to a prismatic joint in which, piston and piston rod is sliding inside the

cylinder and movement is restricted by the internal hydraulic pressure of the cylinder which will generate compliance in the leg. Simulation of the various gait performed by the quadruped is carried out which proves the versatility of the three dimensional model generated. Performance analysis is carried out, between rigid legged and compliant legged robot and also static and dynamic gaits are compared.

The paper is organized in following sequence. In section 2, three dimensional dynamic model of quadruped robot is developed using bond graph. Dynamics of body and leg is discussed in detailed. In section 3, simulation results of trot gait is shown and performance measure between rigid and compliant leg and also between trot gait and amble gait is discussed.

II. Modeling of a Quadruped Robot

Modeling of a quadruped robot consists of modeling of angular and translational dynamics of robot body and legs. Figure 1 shows the schematic diagram of a quadruped robot model in which $\{A\}$ is an inertial frame and $\{B\}$ is the body frame. Frame $\{0\}$ is fixed at the hip joint of each leg which is fixed on the robot body. Each leg of the quadruped robot has two degree of freedom (DOF) with two revolute joints per leg. The joint between links i and i+1 is numbered as i+1. A coordinate frame $\{i+1\}$ is attached to $(i+1)$ joint. A coordinate frame is attached to each link. The link frames are named by a number according to the link to which they are attached i.e. frame $\{i\}$ is rigidly attached to link i. The rotational inertias are defined about frames fixed at the center of gravity (CG) of the link. The CG frame is fixed along the principal directions in the link or body. The surface on which the robot is walking is assumed as a hard surface.

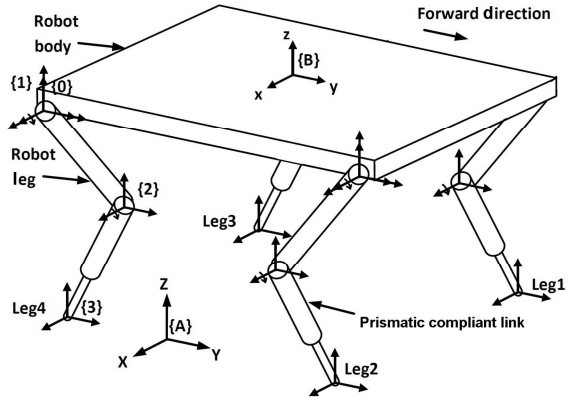

Fig. 1. Schematic representation of quadruped robot with compliant legs

A. Dynamics of a Robot Body

For a given instant, the body has absolute translational velocity v and absolute angular velocity ω. The translational velocity and angular velocity vectors have been resolved into three mutually perpendicular components v_x, v_y, v_z and ω_x, ω_y, ω_z. The net force F acting on the body and the linear momentum p can be related as [18],

$$\vec{F} = \frac{d\vec{p}}{dt} \tag{1}$$

where $p = mv$, if v is expressed with respect to a rotating frame then net force F is given as,

$$\vec{F} = \left(\frac{\partial \vec{p}}{\partial t}\right)_{rel} + \vec{\omega} \times \vec{p} \tag{2}$$

where $\left(\frac{\partial \vec{p}}{\partial t}\right)_{rel}$ is the rate of change of momentum relative to the moving frame. Similarly, the relationship between the net torque τ acting on the body and the angular momentum h can be written as,

$$\vec{\tau} = \frac{d\vec{h}}{dt} \tag{3}$$

Assuming x-y-z axis to be aligned with the principal axes of the body, the angular momentum can be written as $h = I\omega$ in which I is a diagonal matrix of the principal moments of inertia I_{xb} , I_{yb} and I_{zb}. If h is expressed with respect to the rotating frame then net torque τ can be written as,

$$\vec{\tau} = \left(\frac{\partial \vec{h}}{\partial t}\right)_{rel} + \vec{\omega} \times \vec{h} \tag{4}$$

Using the right-hand rule for equations (2) and (4), the component equations can be written as,

$$F_x = m_b \dot{v}_x + m_b \omega_y v_z - m_b \omega_z v_y \tag{5}$$

$$F_y = m_b \dot{v}_y + m_b \omega_z v_x - m_b \omega_x v_z \tag{6}$$

$$F_z = m_b \dot{v}_z + m_b \omega_x v_y - m_b \omega_y v_x \tag{7}$$

and,

$$\tau_x = I_{xb}\dot{\omega}_x + \left(I_{zb} - I_{yb}\right)\omega_y \omega_z \tag{8}$$

$$\tau_y = I_{yb}\dot{\omega}_y + (I_{xb} - I_{zb})\omega_z \omega_x \tag{9}$$

$$\tau_z = I_{zb}\dot{\omega}_z + \left(I_{yb} - I_{xb}\right)\omega_x \omega_y \tag{10}$$

These nonlinear differential equations are known as Euler's equations. The cross product terms can be treated as forces in a set of equations (5), (6) and (7) and as torques in a set of equations (8), (9) and (10). The forces and torques can be added at the respective 1-junctions and using gyrator-ring structures bond graph is generated as presented in [18]. Generated structure is known as Euler Junction Structures (EJS).

B. Dynamics of a Upper Link of Leg

Translational velocity of frame $\{0\}$ of each leg is given by [19],

$${}^{A}\left({}^{A}\vec{V}_0\right) = {}^{A}\left({}^{A}\vec{V}_B\right) + {}^{A}_{B}R\left[-{}^{B}\left({}^{B}\vec{P}_0\right) \times {}^{B}\left({}^{A}\vec{\omega}_B\right)\right] \tag{11}$$

where, ${}^{A}\left({}^{A}\vec{V}_B\right)$ represents the translational velocity of body frame $\{B\}$ with respect to an inertial frame $\{A\}$ and expressed in frame $\{A\}$; ${}^{B}\left({}^{A}\vec{\omega}_B\right)$ represents the angular velocity of body frame $\{B\}$ with respect to inertial frame $\{A\}$ and expressed in frame $\{B\}$; ${}^{B}\left({}^{B}\vec{P}_0\right)$ represents the position vector of frame $\{0\}$ of i^{th} leg with respect to the body CG frame $\{B\}$. It can be expressed as ${}^{B}\left({}^{B}\vec{P}_0\right)_i = \left[r_{ix}\ r_{iy}\ r_{iz}\right]^T$, where '$i$' denotes leg 1 to 4. Here r denotes position of frame $\{0\}$ with respect to body CG frame. In equation (11), ${}^{A}_{B}R$ represent the transformation from body frame $\{B\}$ to inertial frame $\{A\}$ and can be expressed as,

$${}^{A}_{B}R = \begin{pmatrix} c\theta c\emptyset & s\psi s\theta c\emptyset - c\psi s\emptyset & c\psi s\theta c\emptyset + s\psi s\emptyset \\ c\theta s\emptyset & s\psi s\theta s\emptyset + c\psi c\emptyset & c\psi s\theta s\emptyset - s\psi c\emptyset \\ -s\theta & s\psi c\theta & c\psi c\theta \end{pmatrix} \quad (12)$$

where, $c\theta$ is shorthand for $cos\theta$, $s\theta$ for $sin\theta$ and so on. $\emptyset, \theta$ and ψ are the *Z-Y-X* Euler angles. Governing equation for an angular velocity propagation (AVP) of links of a leg can be given as [17],

$${}^{i+1}\left({}^{A}\vec{\omega}_{i+1}\right) = {}^{i+1}_{i}R\ {}^{i}\left({}^{A}\vec{\omega}_i\right) + {}^{i+1}\left({}^{i}\vec{\omega}_{i+1}\right) \quad (13)$$

where, ${}^{i+1}\left({}^{A}\vec{\omega}_{i+1}\right)$ is the angular velocity of $(i + 1)$ link with respect to inertial frame $\{A\}$ and expressed in $(i + 1)^{th}$ frame, ${}^{i}\left({}^{A}\vec{\omega}_i\right)$ is the angular velocity of the i^{th} link with respect to the inertial frame $\{A\}$ and expressed in i^{th} frame and ${}^{i+1}\left({}^{i}\vec{\omega}_{i+1}\right)$ is the angular velocity of $(i + 1)$ link as observed from i^{th} link and expressed in $(i + 1)^{th}$ frame. The term can be expressed for link 1 and 2 respectively as, ${}^{1}\left({}^{0}\vec{\omega}_1\right) = [\dot{\theta}_1 \quad 0 \quad 0]^T$, ${}^{2}\left({}^{1}\vec{\omega}_2\right) = [\dot{\theta}_2 \quad 0 \quad 0]^T$, where $\dot{\theta}_1$represents angular velocity of frame $\{1\}$ with respect to frame $\{0\}$ expressed in frame $\{1\}$ and similarly $\dot{\theta}_2$ represents the angular velocity of frame $\{2\}$ with respect to frame $\{1\}$ expressed in frame $\{2\}$.

For translational velocity propagation (TVP), governing equation for the link tip velocity and link CG velocity are given as,

$${}^{A}\left({}^{A}\vec{V}_{i+1}\right) = {}^{A}\left({}^{A}\vec{V}_i\right) + {}^{A}_{i}R\left[{}^{i}\left({}^{A}\vec{\omega}_i\right) \times {}^{i}\left({}^{i}\vec{P}_{i+1}\right)\right] \quad (14)$$

Where, P refers to the position vector of link frames $\{1\}$, $\{2\}$, $\{3\}$ with respect to its previous frames. Link lengths l_1 and l_2 are taken along the principal *Y*-axis of the links and hence represented in vector form as, ${}^{0}\vec{P}_1 = [0 \quad 0 \quad 0]^T$, ${}^{1}\vec{P}_2 = [0 \quad l_1 \quad 0]^T$, ${}^{2}\vec{P}_3 = [0 \quad l_2 \quad 0]^T$

Equation (14) can be simplified as,

$${}^{A}\left({}^{A}\vec{V}_{i+1}\right) = \left[{}^{A}\left({}^{A}\vec{V}_i\right)\right] + [{}^{A}_{i}R]\left[-{}^{i}\left({}^{i}\vec{P}_{i+1}\right)\times\right]\left[{}^{i}\left({}^{A}\vec{\omega}_i\right)\right] \quad (15)$$

For position of a link CG, ${}^{i}\left({}^{i}\vec{P}_{Gi}\right) = [0 \quad l_{Gi} \quad 0]^T$

$${}^{A}\left({}^{A}\vec{V}_{Gi}\right) = \left[{}^{A}\left({}^{A}\vec{V}_i\right)\right] + [{}^{A}_{i}R]\left[-{}^{i}\left({}^{i}\vec{P}_{Gi}\right)\times\right]\left[{}^{i}\left({}^{A}\vec{\omega}_i\right)\right] \quad (16)$$

Equations (14), (15) and (16) represent the TVP of link in each leg of the robot. The CG velocity of links depends on link inertia. In the bond graph model "*I*" elements (representing mass of a link), are attached at flow junctions. They yield the CG velocities of links. The starting point of the current link is same as the previous link tip. Hence, the tip velocity of the previous link and the angular velocity of the current link are used to find the tip velocity and the CG velocity of the current link. ${}^{i}\left({}^{A}\vec{\omega}_i\right)$ in above equations can be obtained from the AVP for the current link.

The EJS to represent angular dynamics of the link can be constructed similarly as discussed in section 2.1. In case of link, torque is provided in *x* direction only. A pad is used to avoid differential causality. Pads are artificial compliances/lumped flexibilities that can be used in bond graph [20, 21]. Bond graph model of above discussed body and leg dynamics is developed in SYMBOLS software [22]. Nomenclature used throughout paper is listed in Appendix 1.

C. Dynamics of the Prismatic Link

Lower link of the quadruped leg can be considered as a prismatic link, in which piston and piston rod is sliding inside cylinder. The movement is restricted by the internal hydraulic pressure of the cylinder and helical compression spring attached at the piston rod. This arrangement generates compliance in the leg. The sliding of piston is one of the most difficult multi body components which give rise to nonlinear equations of motion. It is important to develop bond graph model of prismatic link with proper mass distribution. Incorrect modeling of entire prismatic link generates improper inertial forces. Thus, utmost care should be taken at the time of generating bond graph model of the three dimensional prismatic link. Bond graph modeling of prismatic link is developed from the concept presented in [23, 24, 25, 26, 27]. The schematic drawing of prismatic link is shown in fig. 2.

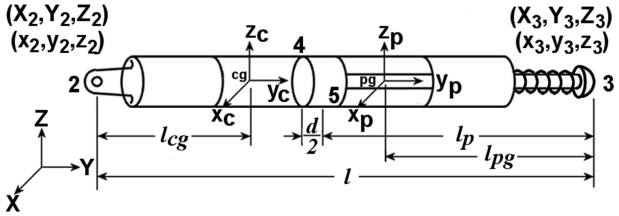

Fig. 2. Schematic diagram of prismatic link

Local coordinate frame is attached at the center of mass of piston (x_p, y_p, z_p) and cylinder (x_c, y_c, z_c) and they are assumed to be aligned with the inertial principal axes. Piston and cylinder motions are described with reference to this body fixed coordinate system which rotate and translate with the respective rigid bodies. The end of the cylinder part will be fixed with the link 1 of quadruped robot and piston end will touch the ground. X_2, Y_2, Z_2 and X_3, Y_3, Z_3 are the inertial coordinate system while x_2, y_2, z_2 and x_3, y_3 ,z_3 are body fixed or non-inertial coordinate

system of the cylinder and piston end respectively. The contemporary length l_c is the distance between the two end points. The center of gravity of the cylinder is located at a distance of l_{cg} from the fixed end. The combined center of gravity of the piston and the rod is located at a distance of l_{pg} from the rod end. The length of the piston is *d*. The center of the piston is located at a distance l_p from the rod end.

The velocity vector of the cylinder in the inertial frame is represented as $v_{Xc,Yc,Zc}$ and in the body fixed frame as $v_{xc,yc,zc}$. The angular velocity vector in the body fixed frame is $\omega_{xc,yc,zc}$. Then, Euler equation for translatory motion of the cylinder can be given as,

$$F_{xc} = M_c\ddot{x}_c + M_c(\dot{z}_c\omega_{yc} - \dot{y}_c\omega_{zc}) \quad (17)$$

$$F_{yc} = M_c\ddot{y}_c + M_c(\dot{x}_c\omega_{zc} - \dot{z}_c\omega_{xc}) \quad (18)$$

$$F_{zc} = M_c\ddot{z}_c + M_c(\dot{y}_c\omega_{xc} - \dot{x}_c\omega_{yc}) \quad (19)$$

where F_{xc}, F_{yc}, F_{zc} are external forces acting in body-fixed x_c, y_c and z_c directions respectively, ω_{xc}, ω_{yc} and ω_{zc} are angular velocities of the mass center of the cylinder in the body fixed frame. $\dot{x}_c$, $\dot{y}_c$ and $\dot{z}_c$ are velocities of the mass center in the body fixed frame, $\ddot{x}_c, \ddot{y}_c$ and $\ddot{z}_c$ are accelerations of the mass center in the body fixed frame. Similarly, Euler equations for rotary motion of the cylinder can be given as,

$$M_{xc} = I_{xc}\dot{\omega}_{xc} - (I_{yc} - I_{zc})\omega_{yc}\omega_{zc} \quad (20)$$

$$M_{yc} = I_{yc}\dot{\omega}_{yc} - (I_{zc} - I_{xc})\omega_{zc}\omega_{xc} \quad (21)$$

$$M_{zc} = I_{zc}\dot{\omega}_{zc} - (I_{xc} - I_{yc})\omega_{xc}\omega_{yc} \quad (22)$$

where I_{xc}, I_{yc} and I_{zc} are second moment of inertia about the principal axes, M_{xc}, M_{yc} and M_{zc} are components of resultant moment due to external forces and couples about the non rotating coordinate frame whose axes are momentarily aligned with the principal axes of the body.

Above Euler equations can be represented by the double gyrator rings where the gyrators are modulated by the angular velocities in the body fixed frame. Similarly, Euler equations can be generated for the piston also and it can be represented by the double gyrator rings. Generated bond graph model of above equations are shown in fig. 3 in which G1 to G12 are the gyrator moduli taken from above equations. The position of the fixed point in the body fixed frame is x_2, y_2, z_2. The velocity of the cylinder in the body fixed frame is

$$\dot{x}_2 = \dot{x}_c + z_2\omega_{yc} - y_2\omega_{zc} \quad (23)$$

$$\dot{y}_2 = \dot{y}_c + x_2\omega_{zc} - z_2\omega_{xc} \quad (24)$$

$$\dot{z}_2 = \dot{z}_c + y_2\omega_{xc} - x_2\omega_{zc} \quad (25)$$

Equations (23), (24) and (25) are body fixed velocities. So, it is necessary to convert it into the inertial frame by coordinate transformation block (CTF). CTF block are generated using successive multiplication of rotation matrices as follows:

$$\begin{Bmatrix}\dot{X}_2\\ \dot{Y}_2\\ \dot{Z}_2\end{Bmatrix} = T_{\emptyset c,\theta c,\psi c}\begin{Bmatrix}\dot{x}_2\\ \dot{y}_2\\ \dot{z}_2\end{Bmatrix} \quad (26)$$

where

$$T_{\emptyset c,\theta c,\psi c} = \begin{bmatrix}c\emptyset_c & -s\emptyset_c & 0\\ s\emptyset_c & c\emptyset_c & 0\\ 0 & 0 & 1\end{bmatrix}\begin{bmatrix}c\theta_c & 0 & s\theta_c\\ 0 & 1 & 0\\ -s\theta_c & 0 & c\theta_c\end{bmatrix}\begin{bmatrix}1 & 0 & 0\\ 0 & c\psi_c & -s\psi_c\\ 0 & s\psi_c & c\psi_c\end{bmatrix} \quad (27)$$

$c\theta_c$ is shorthand for $cos\theta_c$, $s\theta_c$ for $sin\theta_c$ and so on and $\emptyset_c, \theta_c$ and ψ_c are the *Z-Y-X* Cardan angles. Components of $T_{\emptyset c,\theta c,\psi c}$ are used to construct CTF block. Similarly, the velocity of the piston in the body fixed frame can be written and it can be converted into an inertial frame. It is to be noted that the required angle for CTF block are derived from the inverse transformation from body-fixed angular velocities to Euler angle rates [27].

The normal fixed velocities at the contact point 4 and 5 on the cylinder and piston along *x* and *z* directions by assuming a thin but long piston can be given as,

$$\dot{x}_{4c} = \dot{x}_c + \left(l - l_p - l_{cg} - \frac{d}{2}\right)\omega_{zc} \quad (28)$$

$$\dot{z}_{4c} = \dot{z}_c + \left(l - l_p - l_{cg} - \frac{d}{2}\right)\omega_{xc} \quad (29)$$

$$\dot{x}_{4p} = \dot{x}_p - \left(l_p - l_{pg} + \frac{d}{2}\right)\omega_{zp} \quad (30)$$

$$\dot{z}_{4p} = \dot{z}_p - \left(l_p - l_{pg} + \frac{d}{2}\right)\omega_{xp} \quad (31)$$

$$\dot{x}_{5c} = \dot{x}_c + \left(l - l_p - l_{cg} + \frac{d}{2}\right)\omega_{zc} \quad (32)$$

$$\dot{z}_{5c} = \dot{z}_c + \left(l - l_p - l_{cg} + \frac{d}{2}\right)\omega_{xc} \quad (33)$$

$$\dot{x}_{5p} = \dot{x}_p - \left(l_p - l_{pg} - \frac{d}{2}\right)\omega_{zp} \quad (34)$$

$$\dot{z}_{5p} = \dot{z}_p - \left(l_p - l_{pg} - \frac{d}{2}\right)\omega_{xp} \quad (35)$$

where ω indicates the body fixed angular velocity about the axis indicated in subscript. Subscript *c* has been used for cylinder while *p* has been used for the piston. The rate of change of contemporary length between two end points of prismatic link can be expressed as

$$\dot{l}_c = \left(\frac{X_2 - X_3}{l_c}\right)(\dot{X}_2 - \dot{X}_3) + \left(\frac{Y_2 - Y_3}{l_c}\right)(\dot{Y}_2 - \dot{Y}_3) + \left(\frac{Z_2 - Z_3}{l_c}\right)(\dot{Z}_2 - \dot{Z}_3) \quad (36)$$

As shown in fig. 3, μ_x, μ_y and μ_z moduli are used to derive the relative sliding velocity between piston and cylinder at a '0' junction, compliance in the link is

modeled by ‘C’ and ‘R’ element. For contact point mechanics, to compute contact point velocities in body fixed frame moduli R_1 to R_4 and R_5 to R_8 are determined from kinematic analysis of the cylinder and piston respectively. Through a set of transformer moduli μ_1 to μ_{12} similar to an expanded form of CTF block, body fixed velocities are transformed into inertial velocities and then they are implicitly constrained. The relative normal velocity between the contact point on the cylinder and the normal velocity at the contact point on the piston are implicitly constrained by contact stiffness and damping parameters, k_b and R_b respectively.

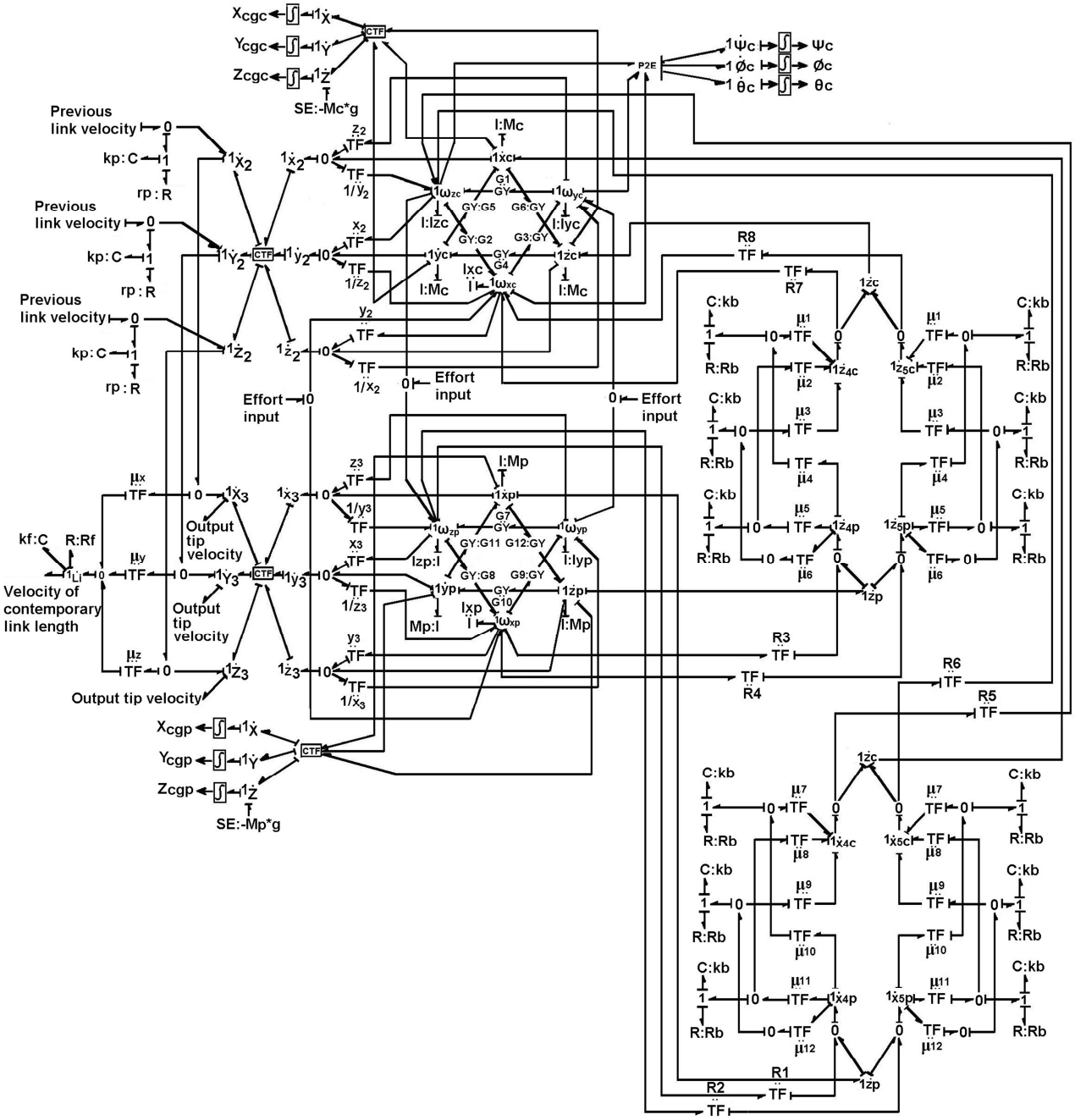

Fig. 3. Bond graph model of prismatic link

D. Dynamics of Combined Body and Leg Links

The bond graph model is developed using above discussed body and leg dynamics. A compact and a simple presentation of a bond graph model can be carried out in multi bond graph form. Here also developed three dimensional model of quadruped robot is presented in multi bond graph form as shown in fig. 4. TVP sub-model is shown in the ‘Body’ part of the multi bond graph. It takes the angular velocity from a body ${}^{V}({}^{A}\vec{\omega}_{B})$ (obtained from EJS) and translational velocity ${}^{A}({}^{A}\vec{V}_{B})$ (decided by body mass) as input and gives out the velocity of {0} frame to the link 1 of each leg. Frame {0} and {1} are coincident for each leg. Hence, the velocity of frame {1} is same as the frame {0}. ‘Leg’ sub model in the multi bond graph represents a two DOF leg. It takes the angular and

linear velocity of body and joint torques about *X*-axis as input. It uses AVP and TVP sub-models of links 1 and 2 and gives out leg tip velocity as output. This sub-model furnishes complete dynamics of a two link leg. The various sub-models shown in fig. 4 for leg 1 can also be used to model leg 2, 3 and 4. The leg tip sub-model in fig. 4 represents the modeling of leg tip-ground interaction. An '*R*' element is appended to '1' junction of each leg in the *X* and *Y* direction, to model the frictional resistance offered by ground while the 'C' element is used to model compliance. Similarly, '*C*' and '*R*' elements are attached in *Z* direction to model the normal reaction force from the ground. Leg tip position sensors in each direction yields the leg tip position coordinates. A systematic construction of bond graph model yields a dynamics expression that can be written in matrix form as

$$\tau_i = \left[A(\theta)\ddot{\theta} + B\left(\theta,\dot{\theta}\right) + C(\theta)\right]_i - J_i^T F_i \qquad (37)$$

where, τ is the 2x1 matrix of joint torque and *F* is the 3x1 vector of the ground contact force of leg *i*, *J* is the Jacobian matrix, *A*(*θ*) is the 3x3 is the mass matrix, *B* is a 3x1 matrix of centrifugal and Coriolis terms and *C*(*θ*) is a 3x1 matrix of gravity terms.

Compliance in the link improves locomotion of quadruped robot. But over compliance reduces locomotion speed and increases posture disturbance. So, optimum design of compliance is must for specific robot configuration. This objective can be achieved by simulating generated bond graph model of quadruped. Number of simulations can be carried out by varying the stiffness and resistance, and its values can be finalized for maximum locomotion speed of robot. This optimum stiffness and load coming on each leg becomes the key parameters for designing the spring used in prismatic link. Number of turn of spring '*n*' can be decided as

$$n = \frac{\delta G d}{8 W C^3} \qquad (38)$$

where, *W* is load, *δ* is axial deflection derived from load(W)/stiffness(*K*), *C* is spring index derived from coil diameter(*D*)/wire diameter(*d*) and *G* is the Modulus of rigidity of spring material.

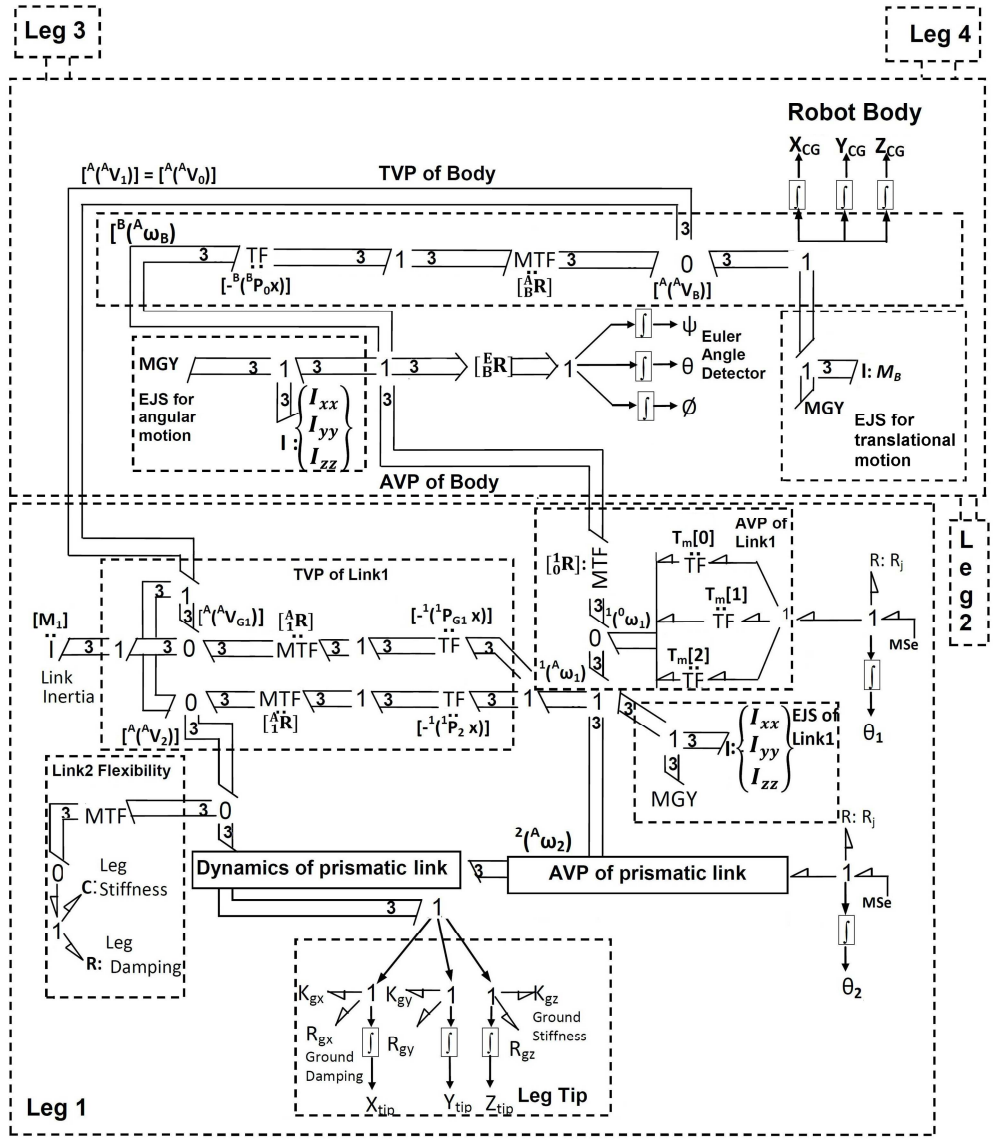

Fig. 4. Multi bond graph of a quadruped robot

III. SIMULATION AND RESULTS

A. Joint rotation for locomotion

Walk can be classified as "static walk" and "dynamic walk". In static walk stability is maintained by keeping, at least three feet planted on the ground and maintaining the center of gravity within the support polygon. In dynamic walk stability is maintained by continuously moving either the feet or the body to maintain balance. Alexander [26] shows various gait pattern followed by four legged animal. Here statically stable gait 'Amble' and dynamically stable gait 'trot' is considered for validation of dynamic model. As shown in fig. 5 diagonal legs are operated together in case of trot gait, while in amble gait legs are operated one by one in 1-4-2-3 sequence. Now, to run the bond graph model in any of the gait, it is necessary to know rotation required at each joint so that a required voltage can be supplied to get the desired rotation of a joint. Thus, to determine a joint rotation for leg forward and body forward movement, graphical presentation is carried out. Graphical presentation as shown in fig. 6 gives an idea about a joint rotation required for the said movement. From this, joint position with reference to time is listed in Table 1 for trot gait. Here, cubic curve is fitted for smooth joint rotation. The required voltage for the said movement is supplied by actuator which is controlled by PD controller.

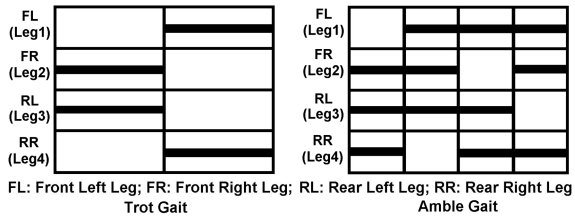

Fig. 5. Trot and Amble gait

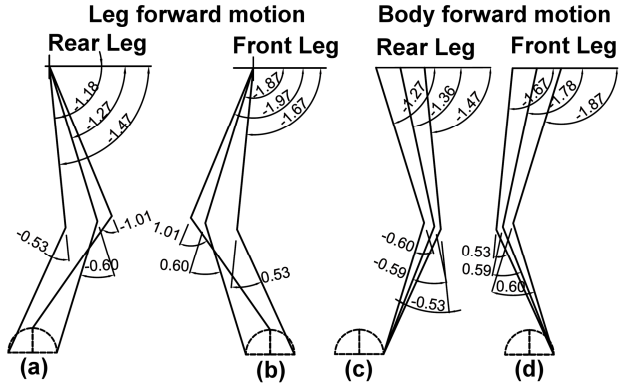

Fig. 6. Graphical presentation of leg and body movement

TABLE I. JOINT POSITION FOR TROT GAIT

Joint position corresponding to time interval	Leg 1		Leg 2		Leg 3		Leg 4	
	Joint 1	*Joint 2*	*Joint 1*	*Joint 2*	*Joint 1*	*Joint 2*	*Joint 1*	*Joint 2*
Initial joint angle	-1.87	0.6	-1.67	0.53	-1.27	-0.6	-1.47	-0.53
$T_o \le t < T_1/2$	-1.97	1.01	-1.78	0.59	-1.36	-0.59	-1.18	-1.01
$T_1/2 \le t < T_1$	-1.67	0.53	-1.87	0.6	-1.47	-0.53	-1.27	-0.6
$T_1 \le t < T_2/2$	-1.78	0.59	-1.96	1.01	-1.18	-1.01	-1.36	-0.59
$T_2/2 \le t < T_2$	-1.87	0.6	-1.67	0.53	-1.27	-0.6	-1.47	-0.53

B. Simulation Results

Bond graph model developed in section 2 is simulated for trot gait for which controlled efforts are supplied to the actuator to reach to required joint position shown in Table 1. Input parameter considered for the simulation is listed in Table 1 of Annexure 2. Positive *Y* direction is considered as forward direction. Each cycle is of 0.5 s. Simulation is carried out for five cycles, result of which is shown in fig. 7. Each leg tip movement in *Z* and *Y* direction and body CG movement in *X*, *Y* and *Z* direction are shown in fig. 7. It shows robot moves in a forward direction. An initial disturbance in body CG *Z* direction is observed because of compliance in the leg and then pattern stabilizes. Similar way, simulation can be carried out for other gait also.

C. Performance measure

Efficient dynamic model plays a vital role in research of walking robot. The above developed bon graph model can be used for various research aspect related to quadruped. Here, we are demonstrating it with one of them. Robot walk may be evaluated by stability, maximum speed and energy consumption. Parameters like a type of gait, stride length, duty factor, length of leg, joint angle and rotation are deciding the above-mentioned performance criteria. To discuss advantage and disadvantage of different designs and control strategies, it is necessary to evaluate and compare robot performance and abilities with respect to common criteria. A common measure to evaluate and compare the energy efficiency of vehicles is the energy consumption per unit distance. To justify the comparison, mass moved and velocity obtained should also be considered with the cost of locomotion. We are comparing here quadruped walk with specific resistance ($\in$). The specific resistance [29, 30] is a dimensionless number describing the energy efficiency of a mobile system. The specific resistance is used as a function of velocity, as

$$\in = \frac{P(v)}{mgv} \tag{38}$$

where, $P(v)$ is the power needed to move the body with velocity v, m is the total mass of the system, and g the acceleration due to gravity.

First, comparison is made between rigid legged and compliant legged quadruped performance. Gait is trot in both the case. Compliant legged quadruped's performance data are taken from above simulation result which says quadruped travels 0.252 m in 2.5 s, means it moves with 0.101 m/s speed. Now to get rigid legged quadruped's performance data, above discussed model is modified and second link of a leg is modeled as rigid instead of

prismatic. We have simulated a rigid legged model with the same speed i.e. 0.101 m/s by tuning controller parameter and final result obtained in terms of body CG displacement in *Y* direction is shown in fig. 8(a). Sensors are placed at the actuator in both the bond graph model which gives power consumption data. The specific resistance equation (38) is evaluated for both the case with robot mass as 3.5 kg, and gravitational acceleration 9.81 m/s^2, which brings specific resistance for the compliance legged model is 2.94 while for rigid legged model 12.91. Smaller the specific resistance, higher the energy efficiency. So from above result, it seems that specific resistance of compliant legged model is smaller, thus, it is energy efficient than rigid legged robot.

Second comparison is made between trot gait and amble gait. The trot gait is considered as a dynamically stable gait, while the amble gait is considered as a statically stable gait. The compliant legged model is simulated for both the gait. Here also results are compared for the same speed. The amble gait takes 0.9 s to complete one cycle. When it is simulated for five cycles, it is found that robot travels 0.2504 m distance with 0.0556 m/s speed. Then, the trot gait is also simulated for the same speed by tuning controller parameter. Body CG displacement obtained in *Y* direction for amble gait is shown in fig. 8(b) and for trot gait is shown in fig. 8(c). Results obtained are used to evaluate equation (38) which brings specific resistance of the trot gait as 2.09 while specific resistance of the amble gait is 7.54. From this result it seems that specific resistance of the trot gait is smaller. Thus the trot gait is energy efficient than the amble gait.

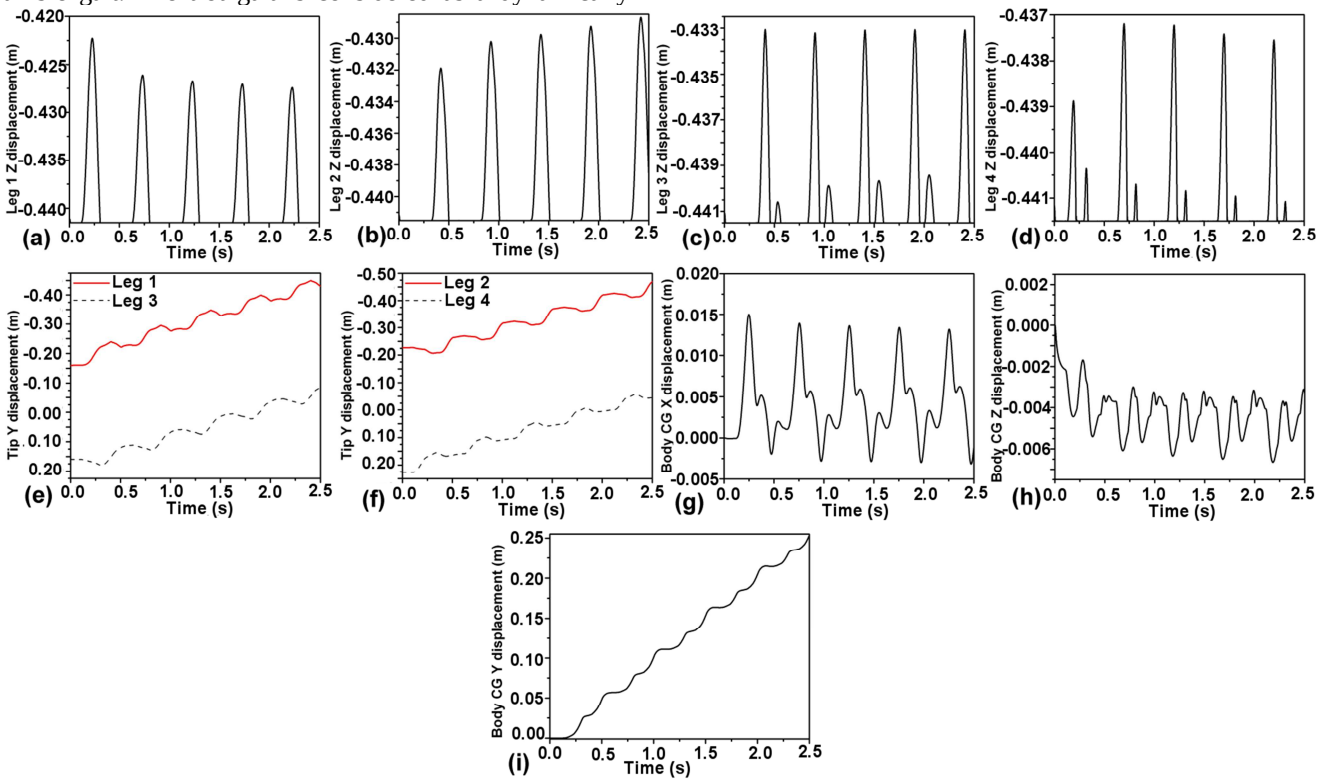

Fig. 7. Time vs. leg tip and body CG movement of compliant legged robot in trot gait

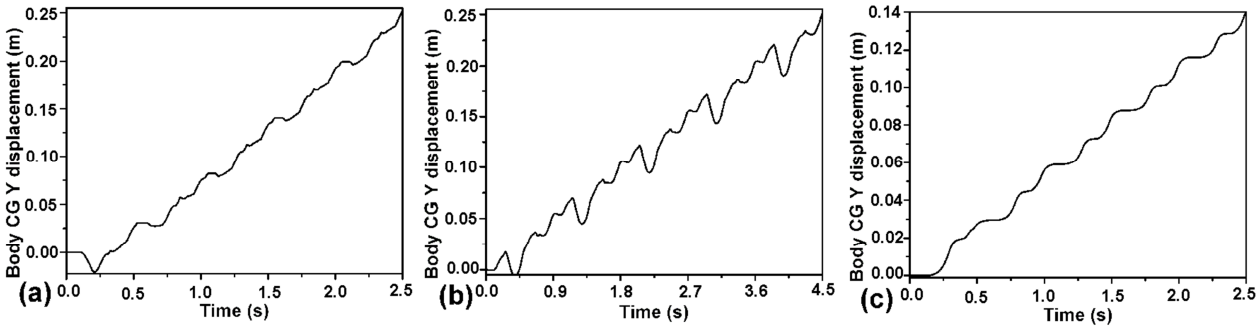

Fig. 8. Body CG *Y* displacement in various conditions

IV. CONCLUSION

A three dimensional model of compliant legged quadruped robot using bond graph has been developed. Generated model is useful for the various research aspects pertaining to quadruped. Performance analysis is carried out, which proves that for the same parameter compliant legged robot is energy efficient than rigid legged robot. It is also concluded that a dynamically stable trot gait is energy efficient than a statically stable amble gait. Developed model will be used for further analysis of different behavior and parameter study of quadruped.

ACKNOWLEDGMENT

The work of M.M. Gor, P. M. Pathak, and A. K. Samantaray has been funded by DST, India under Indo–Korea Joint Research in Science and Technology vide Grant No. INT/Korea/P–13. The work of J.–M. Yang and S. W. Kwak was supported by the National Research Foundation of Korea grant funded by the Korea government (MEST) (No. NRF–2011–0027705).

REFERENCES

[1] D.J. Todd, Walking machines, an introduction to legged robots, Koran Page, London, 1985

[2] M.H. Raibert, Legged robots that balance, MIT Press, Cambridge, MA, 1986

[3] A. Sprowitz, A. Tuleu, M. Vespignani, M. Ajallooeian, E. Badri, and A.J. Ijspeert, "Towards dynamic trot gait locomotion design control and experiments with cheetah-cub, a compliant quadruped robot", The International Journal of Robotics Research, vol. 0, no. 0, 2013, pp. 1-19

[4] K.C. Galloway, J.C. Clark, and D.E. Koditschek, "Variable stiffness legs for robust, efficient, and stable dynamic running", Journal of Mechanisms and Robotics, vol. 5, 2013, pp.011009(1-11)

[5] J.M. Hollerbach, "A recursive lagrangian formulation of manipulator dynamics and a comparative study of dynamics formulation complexity", IEEE Trans. Systems, Man, and Cybernetics, vol. 10, no.11, 1980, pp. 730-736.

[6] W.W. Armstrong, "Recursive solution of the equations of motion of an n-link manipulator", Proceedings of the Fifth World Congress on the Theory of Machines and Mechanisms, Montreal, Canada, vol. 2, 1979, pp. 1342- 1346

[7] M.W. Walker, and D.E Orin, "Efficient dynamic computer simulation of robotic mechanisms", Journal of Dynamic Systems, Measurements, and Control, vol. 104, 1982, pp. 205-211.

[8] K.S. Anderson, Recursive derivation of explicit equations of motion for efficient dynamic/control simulation of large multibody systems. Ph.D. Dissertation, Stanford University, 1990.

[9] D.E. Rosenthal, "An order n formulation for robotic systems", Journal of Astronautical Sciences, vol. 38, no. 4, Dec. 1990, pp. 511-529.

[10] A.K. Banerjee, "Block-diagonal equations for multibody elastodynamics with geometric stiffness and constraints", Journal of Guidance, Control, and Dynamics, vol. 16, no. 6, Nov.-Dec. 1993, pp. 1092-1100.

[11] D.S. Bae and E.J. Haug, "A Recursive Formation for Constrained Mechanical Systems Dynamics: Part I, Open Loop Systems", Mechanisms, Structures, and Machines, vol. 15, no. 3, 1987, pp. 359-382.

[12] M. Bennani and F. Giri, "Dynamic modelling of a four legged robot", Journal of Intelligent and Robotic Systems, vol. 17, 1996, pp. 419-428

[13] A. Mahapatra and S.S. Roy, "Computer aided dynamic simulation of six legged robot", International Journal of Recent Trends in Engineering, vol. 2, no. 2, 2009, pp. 146-151

[14] V.L. Krishnan, P.M. Pathak, L. Sardana, and S.C. Jain, "Simulation And Experimental Studies on Walking Robot with Flexible Legs", in proceeding of 4th International Conference on Integrated Modeling and Analysis in Applied Control and Automation (IMAACA 2010), Fes, Morocco, 2010, pp. 11-19.

[15] S. Soyguder and H. Ali, "Computer simulation and dynamic modeling of a quadrupedal pronking gait robot with SLIP model", Computers and Electrical Engineering, vol. 28, 2012, pp. 161-174

[16] S.V. Shah, S.K. Saha, and J.K. Dutt, "Modular framework for dynamic modeling and analyses of legged robots", Mechanism and Machine Theory, vol. 49, 2012, pp. 234 –255

[17] Ganesh K. and P.M. Pathak, "Dynamic modelling & simulation of a four legged jumping robot with compliant legs", Robotics and Autonomous Systems, vol. 61, 2013, pp. 221-228

[18] D.C. Karnopp, D.L. Margolis, and R.C. Rosenberg, System Dynamics: Modeling and Simulation of Mechatronic Systems, Fourth edition, New Jersey, 2006 (John Wiley & Sons).

[19] J.J. Craig, Introduction to robotics mechanics and control. 3rd ed. USA, 2005 (Pearson Education)

[20] A.K. Ghosh, A. Mukherjee, and M.A. Faruqi, "Computation of driving efforts for mechanisms and robots using bond graphs", Transactions of the ASME Journal of Dynamic, Systems, Measurement, and Control, vol. 113, no. 4, 1991, pp. 744-748

[21] P.M. Pathak, A. Mukherjee, and A. Dasgupta, "Impedance control of space robots using passive degrees of freedom in controller domain", Transactions of ASME, Journal of Dynamic Systems, Measurement, and Control., vol. 127, no. 4, 2005, pp. 564-578

[22] A.K. Samantaray and A. Mukherjee, User manual of SYMBOLS, High Tech Consultants, S.T.E.P., Indian Institute of Technology, Kharagpur, 2000

[23] T.K. Bera, A.K. Samantaray, and R. Karmakar, "Bond graph modeling of planar prismatic joint", 14th National Conference on Machines and Mechanisms (NaCoMM-09),NIT, Durgapur, India, December 17-18, 2009 , pp. 22-26

[24] T. Ersal, H.K. Fathy and J.L. Stein, "Structural simplification of modular bond-graph models based on junction inactivity", Simulation Modelling Practice and Theory, vol. 17, 2009, pp. 175-196.

[25] T.K. Bera, A.K. Samantaray, and R. Karmakar, "Bond graph modeling of planar prismatic joints", Mechanism and Machine Theory, vol. 49, 2012, pp. 2-20

[26] T.K. Bera, R. Merzouki, B.O. Bouamama, and A.K. Samantaray, "Force control in a parallel manipulator through virtual foundations", Proceedings of the Institution of Mechanical Engineers, Part I: Journal of Systems and Control Engineering, vol. 0, no. 0, 2012, pp. 1–16

[27] R. Merzouki, A.K. Samantaray, P.M. Pathak and B.O. Bouamama, Intelligent Mechatronic Systems - Modeling, Control and Diagnosis, 2013 (Springer-Verlag London)

[28] R.McN. Alexander, "The Gaits of Bipedal and Quadrupedal", The International Journal of Robotics Research, vol. 3, no. 2, 1984, pp. 49-59

[29] G. Gabrielli and T.H. Von Karman, "What price speed?" Mechanical Engineering, vol. 72, no. 10, 1950, pp. 775-781

[30] P. Gregorio, M. Ahmadi, and M. Buehler, "Design, control, and energetics of an electrically actuated legged robot", IEEE Trans. on Systems Man and Cybernetics, vol. 27, no. 4, 1997, pp. 626–634

APPENDIX 1

Nomenclature

$\{A\}$	Inertial frame
$\{B\}$	Robot body frame
c_i, s_i	$\cos(\theta_i)$, $\sin(\theta_i)$
d	Width of a piston of a prismatic link

F	Force
F_{xc}, F_{yc}, F_{zc}	External force acting at the cylinder body fixed x, y and z axes
h	Angular momentum
i	Link number, frame number
I_{rot}	Rotor inertia
I_{xb}, I_{yb}, I_{zb}	Moment of inertia of the robot body about x, y, and z axes
I_{xx1}, I_{yy1}, I_{zz1}	Moment of inertia of the upper link of robot leg about x, y and z axes
I_{xxc}, I_{yyc}, I_{zzc}	Moment of inertia of the cylinder part of a prismatic link about x, y and z axes
I_{xxp}, I_{yyp}, I_{zzp}	Moment of inertia of the piston part of a prismatic link about x, y and z axes
k_b	Contact point stiffness at the piston cylinder of prismatic link
k_f	Flexibility due to hydraulic pressure inside the cylinder of prismatic link
K_{gx}, K_{gy}, K_{gz}	Ground contact stiffness in x, y, and z direction
K_I	Integral gain of controller
K_P	Proportional gain of controller
l_c	Contemporary length of prismatic link
l_{cg}	Distance of cylinder CG from a cylinder end frame of prismatic link
l_i	Length of link i
l_p	Length of a piston and piston rod of prismatic link
l_{pg}	Distance of piston CG from a piston end frame of prismatic link
L_m	Motor inductance
m_b	Mass of the body
m_c	Mass of cylinder part of the prismatic link
m_{li}	Mass of link i
m_p	Mass of a piston and piston rod of a prismatic link
M_{xc}, M_{yc}, M_{zc}	External moment acting at the cylinder body fixed x, y, and z axes
n	Gear ratio
p	Translational momentum
${}^{A}_{B}R$	Transformation from body frame $\{B\}$ to inertial frame$\{A\}$
R_b	Contact point resistance at the piston cylinder of prismatic link
R_f	Friction between piston and cylinder of prismatic link
R_{gx}, R_{gy}, R_{gz}	Ground contact resistance in x, y, and z direction
r_{ix}, r_{iy}, r_{iz}	Position of the frame $\{0\}$ of i^{th} leg with respect to the body CG
R_m	Motor resistance
t	Time
v_x,v_y,v_z	Translational velocities of the body
θ_i	Angular displacement of frame i
τ	Torque
ψ, θ, ϕ	Euler angles representing a robot body rotation about x, y, z axis of the body fixed frame
ψ_c, θ_c, ϕ_c,	Cardan angles about x, y, z axis of the moving fixed frame
ω	Angular velocity
ω_{xc}, ω_{yc}, ω_{zc}	Angular velocities of the mass center of the cylinder in the body fixed frame

APPENDIX 2

TABLE I. INPUT PARAMETERS

Parameters	Value
Leg Parameters	
First link length of leg(l_1)	0.225 m
Mass of first link(M_{l1})	0.25 kg
Mass of cylinder part of the prismatic link(M_c)	0.3 kg
Mass of piston part of the prismatic link(M_p)	0.2 kg
Inertia of Link 1	
I_{xx1}	0.00106 kgm^2
I_{yy1}	0.0000125 kgm^2
I_{zz1}	0.00106 kgm^2
Inertia of cylinder part of prismatic link	
I_{xxc}	0.005144 kgm^2
I_{yyc}	0.0000487 kgm^2
I_{zzc}	0.005144 kgm^2
Inertia of piston and piston rod of prismatic link	
I_{xxp}	0.00168 kgm^2
I_{yyp}	0.000025 kgm^2
I_{zzp}	0.00168 kgm^2
Flexibility due to hydraulic pressure inside the cylinder of prismatic link (k_f)	5000 N/m
Friction between the piston and cylinder of a prismatic link (R_f)	188 Ns/m
Contact point stiffness at the piston cylinder of prismatic link (k_b)	100000 N/m
Contact point resistance at the piston and cylinder of prismatic link (R_b)	1000 Ns/m
Length of piston and piston rod of prismatic link l_p	0.1 m
Distance of cylinder CG from a cylinder end frame of a prismatic link (l_{cg})	0.05 m
Distance of piston CG from a piston end frame of a prismatic link (l_{pg})	0.07 m
Mass of piston & piston rod of the prismatic link (m_p)	0.2 kg
Mass of cylinder part of the prismatic link (m_c)	0.3 kg
Position of the cylinder end point with respect to the body fixed frame at the mass center	
x_2	0.0 m
y_2	-0.05 m
z_2	0.0 m
Position of the piston end point with respect to the body fixed frame at the mass center	
x_3	0.0 m
y_3	0.07 m
z_3	0.0 m
Common Parameter	
Mass of body (Mb)	0.5 kg
Inertia of Body	
I_{xb}	0.0049 kgm^2
I_{yb}	0.0038 kgm^2
I_{zb}	0.0086 kgm^2
Ground damping in x, y, z direction (R_{gx}, R_{gy}, R_{gz})	1000 Ns/m
Ground stiffness in	
x direction (K_{gx})	10000 N/m
y direction (K_{gy})	1 N/m
z direction (K_{gz})	1000000 N/m
Controller Parameter	
Proportional gain of controller (K_P)	30
Derivative gain of controller (K_V)	2.5
Actuator Parameter	
Motor constant (K_m)	0.01Nm/A
Motor armature resistance (R_m)	0.1 Ohms
Motor inductance (L_m)	0.001 H
Rotor inertia	0.0000025 kgm^2
Gear ratio (n)	230